



## Research paper

## Large Crater Clustering tool



Jason Laura\*, James A. Skinner Jr., Marc A. Hunter

U.S. Geological Survey, Astrogeology Science Center, 2255 N. Gemini Dr., Flagstaff, AZ 86001, United States

## ARTICLE INFO

## Keywords:

Planetary science  
GIS  
Clustering  
DBScan  
Impact craters  
ArcMap  
Spatial analysis  
Astrogeology  
Computer science

## ABSTRACT

In this paper we present the Large Crater Clustering (LCC) tool set, an ArcGIS plugin that supports the quantitative approximation of a primary impact location from user-identified locations of possible secondary impact craters or the long-axes of clustered secondary craters. The identification of primary impact craters directly supports planetary geologic mapping and topical science studies where the chronostratigraphic age of some geologic units may be known, but more distant features have questionable geologic ages. Previous works (e.g., McEwen et al., 2005; Dundas and McEwen, 2007) have shown that the source of secondary impact craters can be estimated from secondary impact craters. This work adapts those methods into a statistically robust tool set. We describe the four individual tools within the LCC tool set to support: (1) processing individually digitized point observations (craters), (2) estimating the directional distribution of a clustered set of craters, back projecting the potential flight paths (crater clusters or linearly approximated catenae or lineaments), (3) intersecting projected paths, and (4) intersecting back-projected trajectories to approximate the local of potential source primary craters. We present two case studies using secondary impact features mapped in two regions of Mars. We demonstrate that the tool is able to quantitatively identify primary impacts and supports the improved qualitative interpretation of potential secondary crater flight trajectories.

## 1. Introduction

Planetary mapping and topical science studies rely upon the temporal partitioning of discrete geologic units in order to understand the processes that drove the evolution of the surface. Impact crater size-frequency distributions and cross-cutting relationships jointly provide the data necessary to perform relative surface dating (e.g., Tanaka, 1986; Barlow, 1988; Platz et al., 2013; Tanaka et al., 2014). However, the interpretation of both relative and model absolute crater-based ages is not trivial and often yields conflicting temporal assignments for equivalent geologic units. The accurate quantitative association of primary impact craters (those created by collision of an exogenic impactor with a planetary surface) and secondary impact craters (those created by collision of material ejected from a primary impact on the same body) establishes a compelling ability to not only assess distal stratigraphic associations but also provides a means to explore impact dynamics as related to target material, gravitational fields, and atmospheric effects.

There is expansive literature that explores and summarizes the physics of crater formation, including the excavation and ejection of material from a primary impact and the dynamical circumstances wherein a secondary crater will form. Secondary impact craters have been shown to have maximum diameters that are <5% of the parent

primary diameter (Shoemaker, 1965; Bierhaus et al., 2001), regardless of target body. The secondary crater diameter has been shown to decrease with distance from the primary crater (e.g. McEwen et al., 2005). Closer to the primary crater (<10 crater radii), secondary impact craters tend to be circular to elliptical in shape, have depth/diameter ratios lower than of primary impacts, and commonly display a distinctive chevron, linear, loop, or cluster pattern (Wilhelms et al., 1978, Wilhelms et al., 1987). The computational work described herein relies on the user to identify (i.e., map) potential secondary craters (as points) or crater clusters (as lines). The nuances of such mapping effort are not the focus on this paper but rather the input resulting from such a mapping effort. See Melosh (1989) or McEwen and Bierhaus (2006) for more complete information regarding the cratering process and the characteristics and distributions of secondary craters.

Secondary-to-primary impact relationships have been analyzed for the Moon, Mars, and some Jovian satellites. Wilhelms (1976) leveraged the visual association of both secondary craters and related landforms to larger impact basins on the Moon to help establish a lunar time-stratigraphic scheme. Similarly, Dundas and McEwen (2007) demonstrate that secondary impact craters can be visually mapped back to the source impact using the Lunar crater Tycho. Likewise, Preblich et al. (2007) and McEwen et al. (2005) both report similar findings for the Zunil crater on Mars with McEwen et al. (2005) suggesting that the

\* Corresponding author.

E-mail address: [jlaura@usgs.gov](mailto:jlaura@usgs.gov) (J. Laura).

majority of small-diameter craters (10–200 m) and crater clusters on Mars could be the product of secondary impacts. This assertion is supported by Bierhaus et al. (2005) who suggest that, for Europa, the majority of small craters (95% of all craters with diameters  $\leq$  a few kilometers (km)) are the product of secondary impacts. The differentiation of primary and secondary impact craters significantly affects the use of crater size-frequency distributions as a surface dating mechanism (Shoemaker et al., 1963), particularly at smaller crater diameters. Finally, Bierhaus et al. (2001, 2005) suggest that almost all secondary impacts on the surface of Europa are attributable to a limited number of large primaries.

Focusing more on secondary impact cratering models, Popova et al. (2003, 2007) identify two classes of Martian crater clusters: (1) small clusters with many craters with diameter less than approximately 10 m and spatial extents measurable in the hundreds of meters and (2) large clusters with many craters with diameters of approximately 100 m and spatial extents measurable in kilometers (km). The process for secondary impact creation for the former is attributed to the breakdown of the meteor in the atmosphere and the latter is the product of large, secondary ejections post impact. Both small and large crater clusters can be visually back-projected to potential primary impacts to support the determination of stratigraphic age (Wilhelms et al., 1978). However, visual association between alignments of secondary impact crater chains (and associated landforms) and potential source (primary) impacts alone is not always sufficient for confident spatio-temporal linkage, particularly for those primary impacts that are smaller than basin scales. As such, a much more quantitative method is needed to explore the source-secondary impact relationships.

We leverage the secondary-to-primary relationship and inherent clustering in many secondary crater fields on Mars to demonstrate that the visual back-projection of secondary impact craters can be improved through computational modeling and statistical validation. The resultant secondary-to-primary relationship can then serve as another constraint to extend the stratigraphic record, i.e. surface age, from well determined geologic features such as lunar basins and large Martian impact craters.

Computational modeling of secondary-to-primary impacts provides a critical data product for use in a holistic approach to surface dating with the goal of improving our understanding of planetary geologic processes. This work offers the capability to do four things. First, statistically driven secondary clustering supports pattern identification that might otherwise be lost in the complexity (noise) of temporally layered primary and secondary impacts. Second, the computational identification of the secondary-to-primary relationship supports repeatability and testing of past interpretations and inferences about temporal sequencing of geologic processes upon which these impact-related landforms reside. Next, the ability to automate the search for secondary-to-primary relationships supports future geologic mapping that can depend heavily on chronostratigraphic relationships. Finally, the ability to map secondary-to-primary craters can support the informal identification of a more granular temporal stratigraphic scheme. Collectively, we provide a computational tool with wide science applicability to the planetary geologic community.

The remainder of this work is organized as follows. First, in Section 2 we describe the computational model, including input data sets and the assumptions the model makes. In Section 3 we describe the computational methods used for secondary-to-primary back projections and in Section 4 we apply our methods to the Mare Acidalium and Lunae Palus quadrangles on Mars. Section 6 describes sources of uncertainty in the model. Finally, we conclude with Section 7 and offer areas of potential future work.

## 2. Computational model

The primary contribution of this work is an ArcMap 10.x plugin, written in Visual Basic (VB) dotNET (.NET) that attempts to quantita-

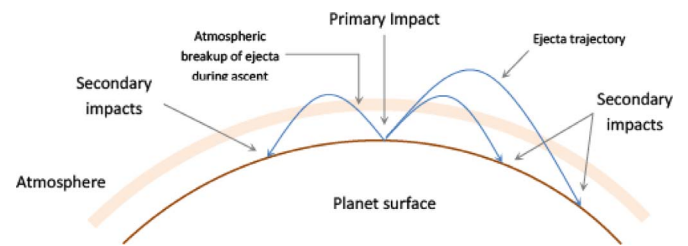


Fig. 1. Overview of the surface processes the LCC toolset seeks to model where secondary impact craters are back-projected along inferred ejecta trajectories to identify potential primary impact craters.

tively relate mapped secondary craters (as points) or crater chains (as lines) to distant primary (source) craters. The presented plugin builds upon previous work by Nava et al. (2009), Nava and Skinner (2010), Skinner and Nava (2011) who prototyped the underlying concepts for a single crater (Zunil) on the Martian surface in ArcGIS 9.x. We call this model the Large Crater Clustering (LCC) tool set. Fig. 1 broadly illustrates the process of primary and secondary impact emplacement. The LCC tool set identifies clusters of secondary impact craters and back projects (along the inferred ejecta trajectory) secondaries seeking to locate primary impact craters while accounting for ejection and orbital properties, of the given planetary body.

### 2.1. Input data sets

The identification of primary impact craters using the developed back-projection method requires the digitization, from remotely sensed data, of secondary impact craters. For the purposes of this tool, we classify secondary impacts into three groups: traditional clusters, crater chains (catenae) and lineated terrains (lineaments). Fig. 2 illustrates the supported data types.

Each input data type (point or line) defines an entry point into the secondary-to-primary modeling process. Broadly, our model functions by extending great circle arcs, that measure orthodromic (spherical) distance, from either the semi-major axis of a bounding ellipse defined by spatial clustering of digitized points or defined linear features. This makes the assumption that clusters have been well defined, either computationally, or manually by the user. The length of these arcs is defined by a user and is a function of post impact ejection speed and flight time. Therefore, digitized points are first statistically clustered using traditional point pattern clustering techniques so that a bounding ellipse can be computed. For line and polygon geometries, great circle arcs can be extended immediately from the ending or semi-major axis points.

### 2.2. Model assumptions

The two primary assumptions made follow Bierhaus et al. (2001). First, secondary craters do not follow the Complete Spatial Randomness (CSR) assumption and instead occur in some identifiable cluster. Second, we assume that large crater clusters are the product of post-impact spallation and ejecta. By extension, the impacting object is also large, resulting in a primary of significant size. In making these assumptions, we also leverage the behavior models developed by Popova et al. (2003, 2007) that are supported by the numerical modeling of Vickery (1986, 1987). That is, large crater clusters are defined by secondaries created by post-impact spallation and ejection of fragments on the order of 5–50 m. Flight times are assumed to generally last between 1000 and 2000 s with the potential for longer 5000 s flights for the largest impacts (Popova et al., 2007). In the latter case, total travel distance, assuming velocities of 3 km/s, and flight times up to 5000 s could be as far as 15,000 km (Popova et al., 2007) with a maximum width dispersion on the order of 25 km (given the radius, gravity, and rotation speed of Mars).

Download English Version:

<https://daneshyari.com/en/article/4965378>

Download Persian Version:

<https://daneshyari.com/article/4965378>

[Daneshyari.com](https://daneshyari.com)